Journal of Structural Geology, Vol. 6, No. 4, pp. 391 to 398, 1984
Printed in Great Britain

0191-8141/84 $03.00 + 0.00

Incremental deformation and fabric development in a KCl/mica mixture

W. D. MEANS

Department of Geological Sciences,
State University of New York at Albany,
Albany, NY 12222, U.S.A.

P. F. WILLIAMS

Department of Geology,
University of New Brunswick,
Fredericton, New Brunswick, Canada E3B5A3

and

B. E. HOBBS

Department of Earth Sciences,
Monash University,
Clayton, Victoria 3168, Australia

(*Received* 7 *October* 1982; *accepted in revised form* 23 *September* 1983)

Abstract—The history of deformation and of mica reorientation is described in a KCl/mica mixture in the middle of a kink-like, experimental shear zone. The history was reconstructed by deforming several specimens to successively greater total strains and assuming the more deformed specimens passed through the states of strain and fabric exhibited by the less deformed specimens.

A pseudo-differentiated layering is described which arises from the original network distribution of the mica grains, without benefit of any differentiation process. A comparison is made between the observed mica fabrics at various strains and those predicted by the March model, taking the measured initial preferred orientation of the micas into account. The actual reorientation processes in the material are found to be more efficient than the March transformation at shortening strains less than about 70% but less efficient at higher strains. These departures from Marchian behavior are explaned qualitatively. Comparison is also made between observed and predicted intensities of mica preferred orientation, assuming a hypothetical random orientation of micas in the starting material for the March calculation.

INTRODUCTION

IN TWO previous papers (Williams *et al.* 1977, Hobbs *et al.* 1982) we described the microstructure and fabric in some experimentally deformed salt/mica specimens, and the relationship of various induced structures to the local state of total finite strain. This paper continues the series with an account of experiments intended to show the history by which the total finite strain accumulates in the material, and the associated history of the mica fabric. The approach has been to deform a series of specimens to successively greater total strains and to assume that the more strongly deformed specimens passed through the states of strain and fabric represented by the less deformed specimens. This incremental or historical approach is valuable in principle because such experiments reveal the details of structural and deformational evolution that are necessary for full understanding of deformation mechanisms, and for investigating the influence of different strain histories upon fabric.

SPECIMENS AND EXPERIMENTAL PROCEDURE

Profile views of the four deformed specimens and an undeformed specimen are shown in Fig. 1. Each specimen is a twelve-layer assembly consisting of two central KCl/mica layers (25% mica by weight), and ten NaCl/mica layers (50% mica by weight). The layers were prepared and rubber-stamped with strain-marker lines in the manner described by Hobbs *et al.* (1982). We focus attention here on deformation and fabric in the central KCl/mica layers. The NaCl/mica layers proved too variable in initial fabric to permit reliable reconstruction of the fabric history.

In the undeformed state the specimens were rectangular blocks measuring 7.9 × 1.9 cm in the plane of the layering by about 2.5 cm normal to the layering. They were deformed dry, at room temperature, inside thick lead jackets with sheets of lead to lubricate the piston faces. The arrangement is shown in Means (1975 fig. 3). The confining pressure was 103 MPa, and the strain rate was 1.2×10^{-4} s^{-1}.

After deformation the specimens were potted in plastic and sawn in half normal to the hinge lines of the folds that developed. Figure 2 shows a view in this plane of specimen 3. The black spots are the strain markers. Their positions were measured in thin section using a micrometer stage, or from photographic enlargements of the sawcut surfaces. Further details of the strain measurement technique are given by Hobbs *et al.* (1982).

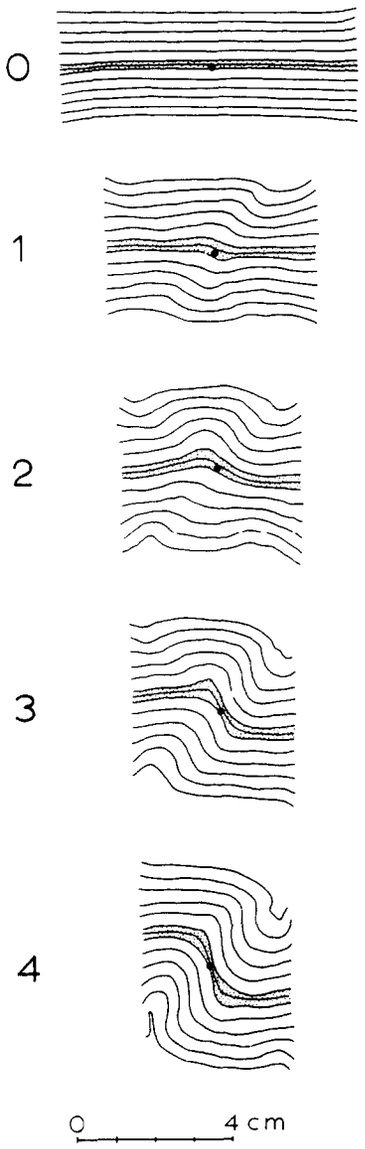

Fig. 1. Profile views of specimens 0–4. Stippled layers are KCl/mica layers. Black dot shows area in center of main kink-like shear zone that was studied in detail.

SPECIMEN-SCALE STRUCTURE

The prominent large-scale structural change in the specimens is the development of a kink-like shear zone that traverses the layers obliquely and widens with increasing overall deformation of the specimens (Fig. 1). Although the shear zone is 'kink-like' in a broad sense and might be identified as a kink band with somewhat rounded hinges if one only saw profile 4 (Fig. 1), its history is not that of an ideal kink in the sense of Paterson & Weiss (1966). In an ideal kink the finite shear strain across the kink stays constant with increasing overall deformation. The kink width grows with time, and this alone accommodates the overall deformation. In the present specimens, however, the shear strain across the kink increases with increasing overall deformation and there is also large concurrent layer-parallel shortening (to the stage represented by specimen 2) in the material outside the kink. These departures from ideal kinking history are represented graphically in Fig. 3.

DEFORMATION HISTORY

Finite strains

Specimens 1, 2, 3, 4 are henceforth referred to as *stages* 1, 2, 3, 4 of a progressive deformation.

The two-dimensional total finite strains at each stage were calculated from measurements of the coordinates of three non-colinear markers in the deformed and undeformed states (see Hobbs *et al.* 1982). This yields the principal stretches s_1 and s_3 in the profile plane of the folds and the angles θ' and θ measured from the s_1 direction to the layering in the deformed and undeformed states.

Calculation of the incremental strains relating each stage to the next was carried out in the same way except now the 'undeformed' coordinates of the three strain markers are the coordinates at the beginning of one of the increments of deformation. These coordinates were calculated from the measured original coordinates (the truly undeformed coordinates) by applying the known finite strain at the start of the increment in question.

There are two sources of error in the strain measurements — the finite size of the strain markers and large-scale inhomogeneity in the strain fields. This led to two sets of strain measurements. Measurements of set A (Table 1) were made using strain markers as far apart as possible in the KCl/mica layers, yet not so far as to enclose very obvious large-scale strain gradients. These markers are shown in Fig. 4. The measurements of set A contain minimum errors due to the finite size of the strain markers, and give orientations (θ) of the s_1 principal strain direction with respect to layering in the undeformed state to within ±2°. No measurement of this type was made for stage 4 because of the unavoidable large strain gradients present. Measurements of set A were used in an attempt to estimate the degree of non-coaxiality of the progressive deformation.

Strain measurements of set B were made using strain markers that are as close together as possible and close to the areas within which the fabric measurements were made (dashed rectangles in Fig. 4). Set B measurements suffer less from the effects of large-scale strain

Table 1

	s_1	s_3	θ'	θ	R
Strain measurements A					
Stage 1	1.7	0.44	—	84°	3.9
Stage 2	2.3	0.35	—	82°	6.6
Stage 3	3.9	0.15	—	81°	26
Strain measurements B					
Stage 1	1.8	0.44	66°	—	—
Stage 2	2.3	0.32	47°	—	—
Stage 3	4.8	0.13	18°	—	—
Stage 4	8.6	0.094	6°	—	—

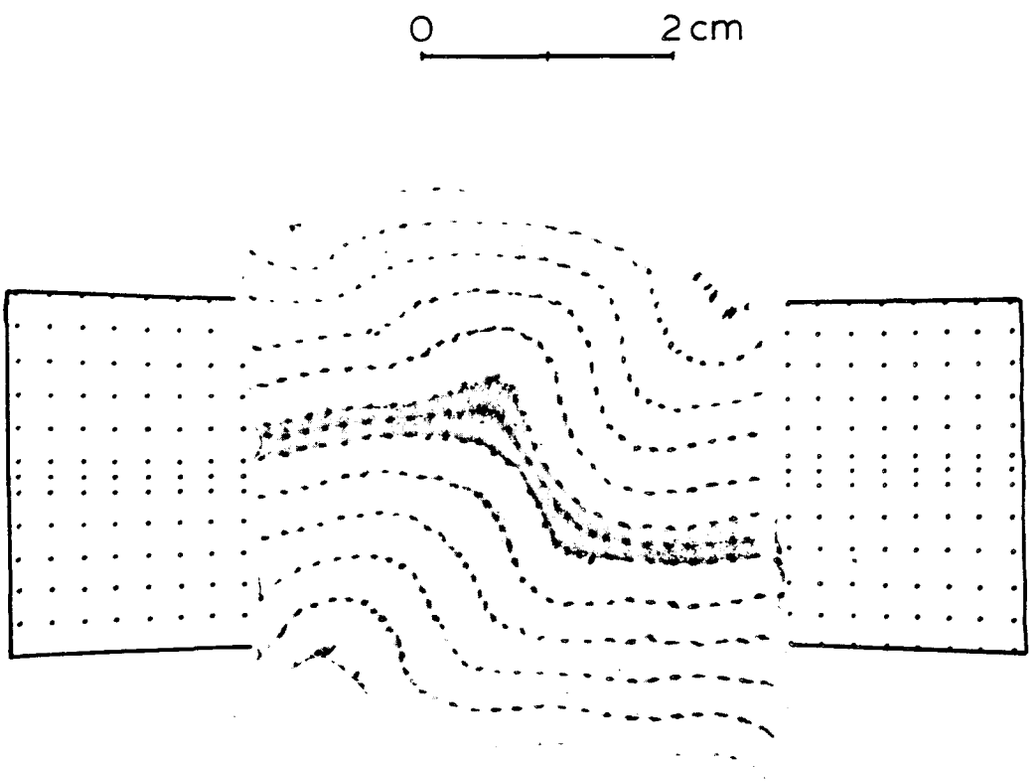

Fig. 2. Photograph of specimen 3 after deformation and its undeformed configuration (line drawing).

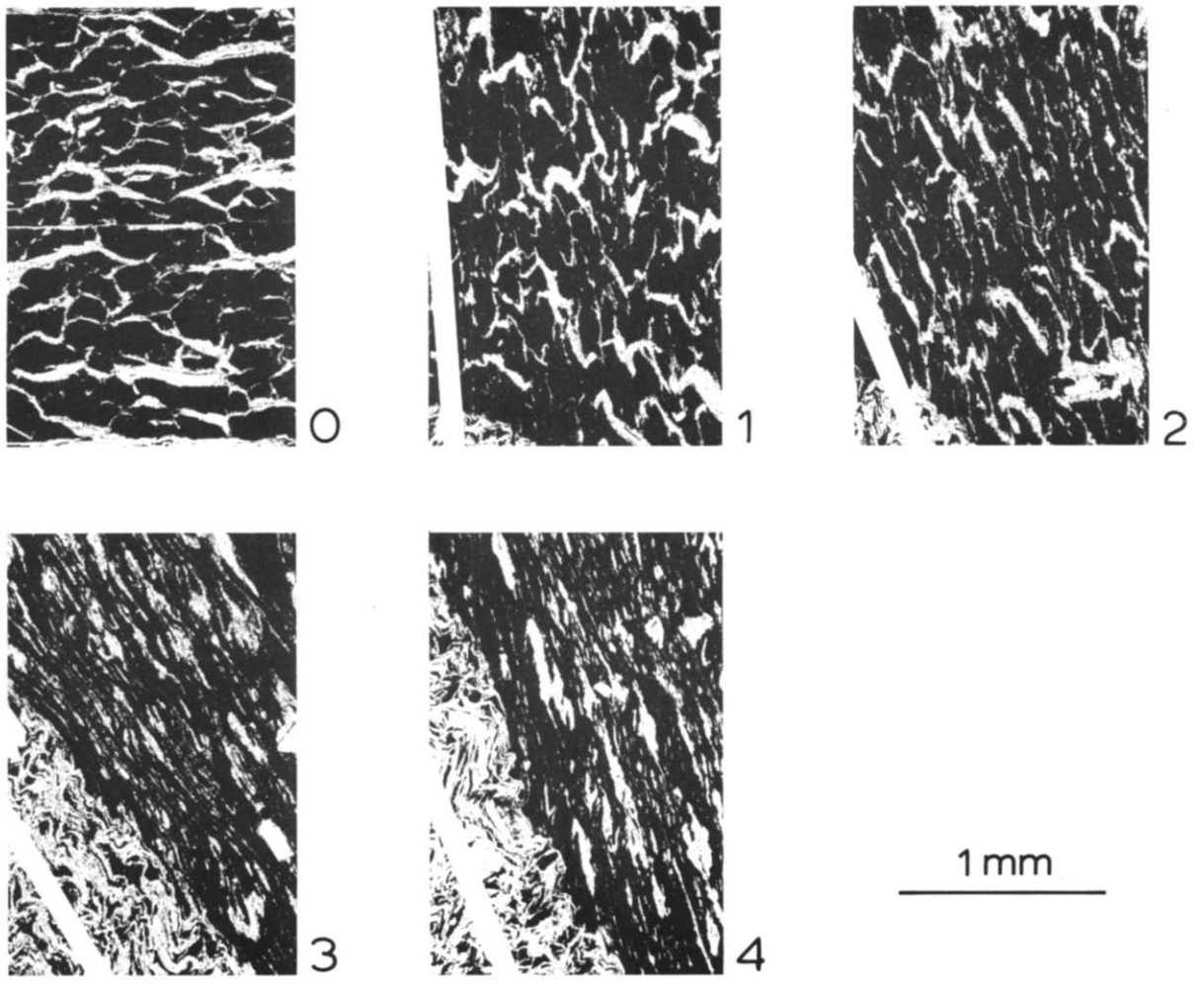

Fig. 5. Photomicrographs of areas in KCl (black)/mica (white) layers within which mica orientations were measured. Positions of these areas are also shown in Fig. 4. White band across lower left corner of photographs 1–4 shows orientation of s_1 direction of total finite strain. Photographs taken with crossed nicols and crossed quarter wave plates so that all micas are illuminated regardless of orientation.

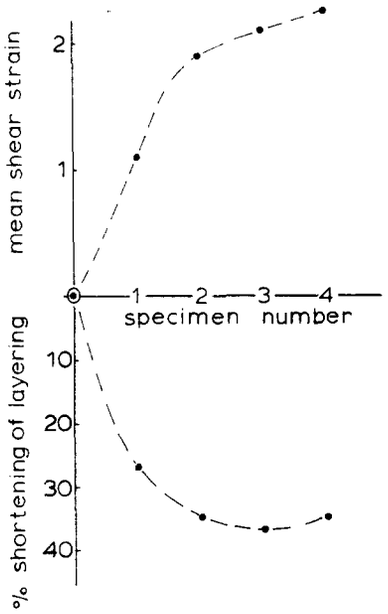

Fig. 3. Departures of specimens from ideal kinking behavior. The mean shear strain across the shear zone increases with increasing overall deformation. The layers outside the zone are shortened substantially while the shear zone develops, to the stage represented by specimen 2. For ideal kinking the mean shear strain across the shear zone would have some constant value for all specimens, and the layering outside the zone would show no shortening for all specimens.

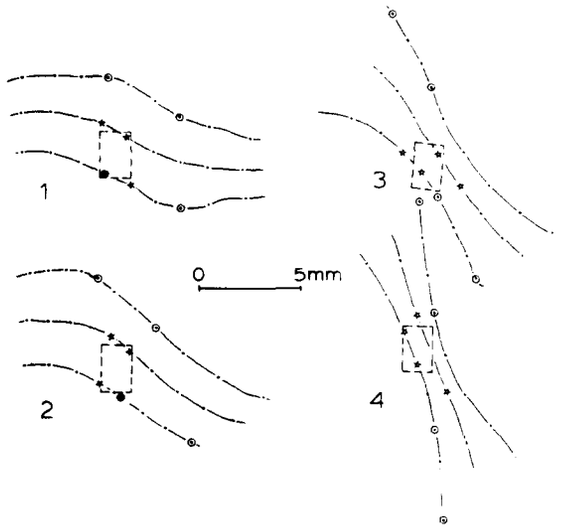

Fig. 4. Enlarged central parts of KCl/mica layers, showing layer boundaries (solid lines) and areas shown in Fig. 5 (dashed rectangles). Strain markers indicated by circles and stars were used respectively to calculate strain parameters of sets A and B (Table 1). Other strain markers shown by dots. Lines connecting the left and right pairs of circled markers on the top and bottom layer boundaries are lines initially orthogonal to the layer boundaries. All drawings in same orientations as Figs. 1 and 5, with the direction of overall shortening horizontal.

inhomogeneity but contain larger errors resulting from the uncertainty in measured positions of the strain markers. The measurements of principal strain directions in set B are good only to ±5°. However, these measurements were considered more appropriate for the comparisons of local strains with local fabrics. Strain parameters of sets A and B are listed in Table 1 and represented graphically by rectangles drawn with their sides parallel and proportional to the principal stretches s_1 and s_3 that lie in the plane of the figures (e.g. Figs. 7 and 9). The quantity R in Table 1 is the axial ratio s_1/s_3 of the strain ellipse.

Degree of non-coaxiality

Some degree of non-coaxiality seems likely in the progressive deformation. The first small increments of strain were probably applied with principal directions parallel and normal to the layering, whereas later increments were applied less symmetrically with respect to the undeformed layering. The only alternative to initially symmetrical straining is the possibility that geometrical irregularities in the layering (of which we were not aware) led to oblique straining even during the first increments of deformation. Some degree of non-coaxiality thus seems probable between Stages 0 and 1, but the experimental data provide no means of measuring it. Between stages 1 and 3 (between 56 and 87% local shortening) we have the pairs of R and θ values shown in Table 1. The nominal small variation of θ with increasing R may or may not be real, considering the ±2° uncertainty in each θ value. An attempt was made to place limits on possible values of the kinematic vorticity number (Means *et al.* 1980) by comparing the observed θ variation with R between stages 1 and 3 with the θ variation calculated for the same range of R values in flows with various constant vorticity numbers. However, M. B. Bayly (pers. comm.) pointed out the danger of using this procedure on experimental flows with vorticity numbers that might have varied with time. In such flows there is no unique relationship between θ variation with increasing R at a given moment and the vorticity number at that moment.

MICA FABRICS

Pseudo-differentiated layering

At the lower strains of stages 1 and 2 a fine micaceous layering is developed (Figs. 5 and 6b). It is approximately parallel to the s_1 principal strain direction and resembles the 'pinstripe' layering familiar in many schistose rocks of medium metamorphic grade. Between the pinstripes are coarser, folded mica grains, of a type which, in rocks, are taken to indicate that the pinstripe foliation is a modified crenulation cleavage. Microstructural details such as those at m and n (Fig. 6b) are normally interpreted to indicate that the crenulation cleavage was modified by some kind of differentiation process. At n (Fig. 6b) a steeply-dipping pinstripe layer cuts across a gently dipping folded layer that would normally be taken to represent the pre-crenulation cleavage foliation. At m a pinstripe layer truncates the gently dipping foliation.

Despite these microstructural relations, the present

200μm

Fig. 6. Details of mica (black) and KCl (white) distribution before and after deformation to illustrate origin of pseudo-differentiated layering. (a) Detail of undeformed material from lower left part of photo 0 in Fig. 5. *M* and *N* mark three- and four-way nodes in the initial network distribution of micas around the KCl grains. (b) Detail of deformed material from lower middle part of photo 2 in Fig. 5. *m* and *n* mark deformed three- and four-way nodes which could give a false impression of an origin by differentiation for the (steeply dipping) 'pinstripe' foliation.

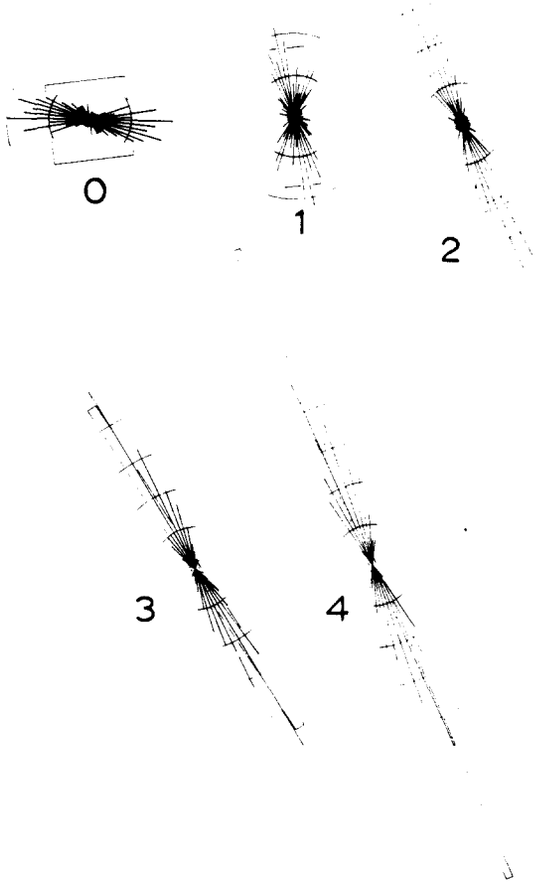

Fig. 7. Circular histograms showing measurements of the trace of (001) of mica and associated strain rectangles for areas 0–4 of Fig. 5. Concentric calibration marks at 0, 5, 10, etc. per cent of total mica. Histogram cell width 5°. 242, 181, 194, 182 and 264 measurements respectively in 0–4 respectively. All strain rectangles to scale given by the unit square of stage 0, drawn with sides parallel to principal directions in undeformed state of first incremental strain of strain measurements B (s_1 at 82° to layering). All drawings in same orientations as Figs. 1 and 5, with overall shortening direction horizontal.

pinstripe layering is clearly not a differentiated crenulation cleavage. The pinstripes are simply very attenuated micaceous regions that were present in the undeformed material and happened to lie in extension orientations. The critical factor for appearance of this type of pinstripe layering is the initial network distribution of the micas (Figs. 5 stage 0 and 6b). Microstructures of types *m* and *n* in the deformed material arise from nodes in the initial network, such as those at *M* and *N* in the undeformed material (Fig. 6a).

Mica orientation and finite strains

Figure 7 shows total strain rectangles for each stage in the deformation and the measured orientations of the trace of (001) of the mica grains. (All mica grains were measured, irrespective of their positions inside or outside the pinstripe layering).

In the undeformed state 0 there is marked preferred orientation approximately parallel to the layering. This was induced during initial compaction of the layers, prior to specimen assembly. It is most marked in the coarser grains.

By stage 1 (56% local shortening) the KCl grains have deformed plastically and the micas have become rotated, in part by folding, to define a bimodal fabric with both modes somewhat oblique to the s_1 direction (Fig. 7 stage 1).

By stage 2 (68% shortening) the KCl grains are more strongly attenuated, the pinstripe layering is well developed, and the mica (001) directions show a unimodal fabric with preferred orientation approximately parallel to the s_1 direction.

By stage 3 (87% shortening) the KCl grains have become extremely attenuated, and the pinstripe layering is less distinct geometrically from the now subparallel foliation defined by the coarse mica grains. The mica preferred orientation has become sharper and again lies parallel to the s_1 direction (with the ±5° uncertainty in the latter). Stage 4 (91% shortening) displays only slight further changes in fabric. In both stages 3 and 4, there are good examples of en échelon coarse mica flakes or 'fish' similar to such features in mylonitic rocks.

Figure 8 shows the intensity of mica preferred orientation as a function of total strain. The intensity measure is the percentage of mica lying with the trace of (001) within 2.5° of the preferred orientation. The strain measure is the percentage shortening in the s_3 direction (from

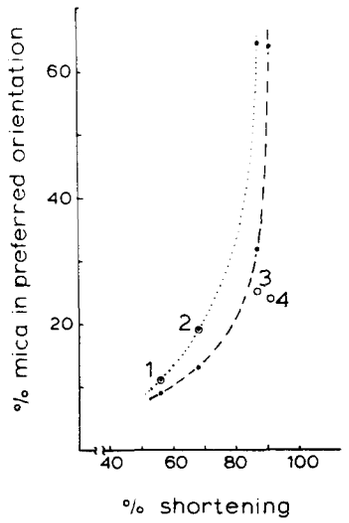

Fig. 8. Intensity of mica preferred orientation plotted against local per cent shortening. Intensity measure is percentage of mica with trace of (001) within 2.5° of the preferred orientation. Circles 1–4 are intensity/strain measurements. Dots on dashed and dotted lines are respectively Marchian predictions assuming observed initial orientation at stage 0 and hypothetical uniform (random) orientation at stage 0.

s_3 values of set B, Table 1). Also shown are intensities predicted by applying the March transformation (March 1932, Owens 1973, Oertel & Wood 1974) to the observed distribution at stage 0 and to a hypothetical uniform distribution at stage 0. For stages 1 and 2 the observed mica concentrations are 20 and 30% stronger than the predicted concentrations employing the real initial preferred orientation parallel to layering. The observed concentrations for stages 1 and 2, however, agree perfectly with the predicted concentrations where a hypothetical uniform orientation is assumed in the starting material. For stages 3 and 4 the observed intensities of mica orientation are considerably weaker than the predicted intensities, particularly where a uniform initial orientation is assumed.

Efficiency of mica reorientation

Figure 8 already suggests that the mica-orienting processes in the KCl/mica material are more efficient than the March 'process' at low and moderate strains but less efficient at shortening strains greater than about 70%. This was investigated further by calculating incremental strains separating each of the stages and applying these to each of the sequentially observed fabrics. The incremental strain generating stage 1 from stage 0 was applied to the observed fabric at stage 0; the incremental strain generating stage 2 from stage 1 was applied to the observed fabric at stage 1, and so on. The results are shown in Fig. 9. There is a bi-modal predicted fabric at stage 1 and unimodal predicted fabrics thereafter, as observed (cf. Figs. 9 and 7). But the predicted fabrics are again weaker than the observed fabrics for stages 1 and 2 while they are stronger than the observed fabrics for stages 3 and 4, confirming the suggestion above that the real orienting process in these materials is more efficient than the March process at lower strains but less efficient at higher strains.

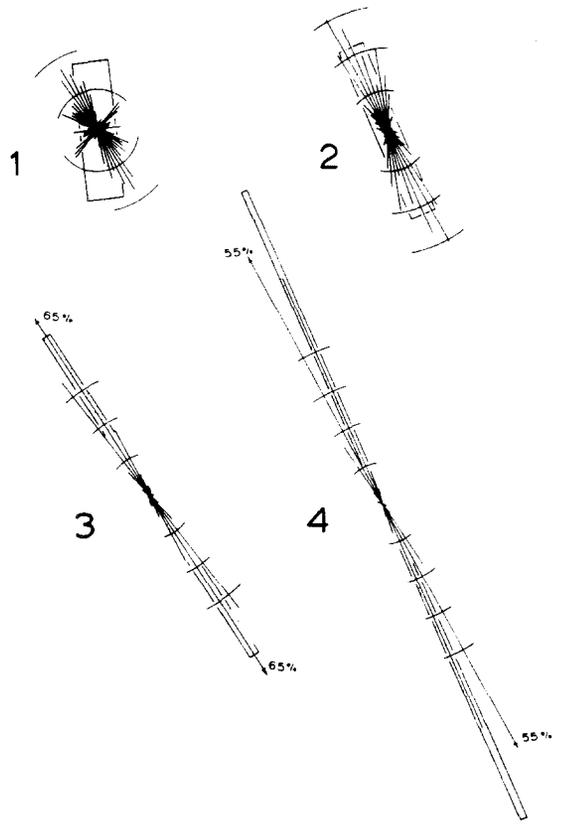

Fig. 9. Marchian predictions comparable with observed mica fabrics shown in Fig. 7, generated incrementally by applying calculated incremental strains to each preceding measured fabric, as explained in text.

DISCUSSION

Distinction between true and pseudo-differentiated layering

In the present material it is easy to identify the origin of the pinstripe layering, because the initial fabric is well known, the strains are known, and the structural development is viewed incrementally. In rocks with such layering, none of this is generally possible, so it becomes a problem to know whether the pinstripe compositional layers were introduced by differentiation during the deformation or whether they are simply a very deformed version of micaceous regions present before deformation. Two criteria for a differentiation origin can be suggested. If a given pinstripe layer contains four or five or more intersections of types *m* or *n* (Fig. 6b), then an origin by differentiation seems attractive. If the micas in the pinstripe layers are compositionally different from those in the crenulated layers, then again an origin by differentiation is perhaps indicated. However, both of these criteria are somewhat unreliable. Many intersections of type *m* (Fig. 6b) might form along a single pinstripe by deformation of an initial micaceous network combined with sliding along sets of boundaries of the non-mica grains that happened to line up. A compositional difference between the crenulated micas and the pinstripe micas might conceivably reflect an original, perhaps sedimentary, difference in compositions

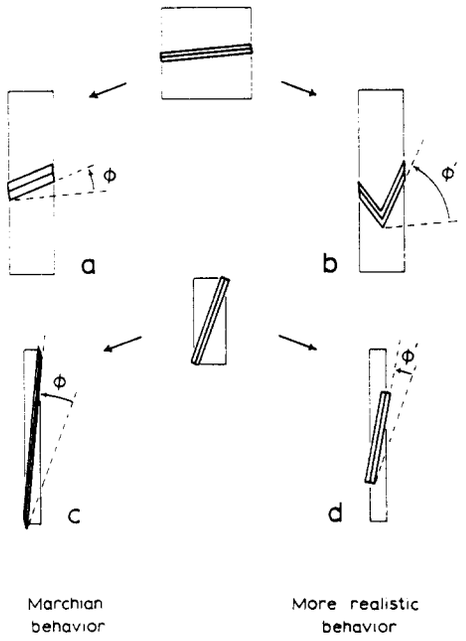

Fig. 10. Contrasted idealized behavior of mica flakes under Marchian transformation (a, c) and in more realistic inhomogeneous deformation (b, d).

between coarse grains which were deposited horizontally in what will become the crenulated foliation and fine grains which settled into and filled up the chinks between the more equant non-mica grains.

Departures from Marchian behavior

The differences between the observed and predicted mica fabrics can be explained qualitatively by considering the nature of the initial fabric in the experiments and the microstructural behavior of the mica flakes. The initial fabric is dominated by micas with the trace of (001) at low angles to the overall shortening direction. In the March transformation such grains contribute little to the new preferred orientation. They shorten and thicken with little rotation (Fig. 10a). In the real material, however, such grains buckle and fold, with large rotations of (001) even at modest strains (Fig. 10b). This small-scale folding, of the grains themselves or of the foliation in which they lie, probably accounts for the greater strength of the observed fabrics (to about 70% shortening) than the predicted fabrics. In rocks behaving this way use of the March model would tend to overestimate the strain that has occurred, if the correct initial fabric is assumed. Yet work by Tullis & Wood (1975), Oertel & Wood (1974) and Wood *et al.* (1976) indicates either good correlation between strains indicated by March analysis and strains indicated by deformed markers, or March strains slightly less than the strains indicated by markers. A possible explanation is that although use of March analysis tends to overestimate strains (in the range of strains commonly encountered in slates), there is a compensating underestimation brought in when the initial fabric is assumed to be uniform or less strongly oriented parallel to bedding than was actually the case. This appears to be the situation illustrated by stages 1 and 2 in our experiments. A qualitatively similar theoretical prediction of low-strain reorientation that is more efficient in anisotropic materials behaving in non-Marchian fashion than in isotropic materials behaving in Marchian fashion is given by Cobbold (1976, fig. 8).

Figures 10 (c) & (d) contrast the observed behavior of mica grains at high strains with the behavior envisioned by March theory. At high strains many grains will have (001) aligned in an extension direction at a low angle to the s_1 direction. March theory assumes such grains are free to extend homogeneously with their matrix and rotate as shown in Fig. 10 (c). In the real material, the grains are not able to extend and the average rotation required by a given increment of deformation will be smaller than in the Marchian case as shown in Fig. 10 (d).

Acknowledgements—This work was supported at various times by N.S.F. Grants GA-15918, EAR 76-03727 and EAR 89-07812. P.F.W. acknowledges partial support from the Netherlands Organization for Advancement of Pure Research (Z.W.O.). The manuscript was improved under criticism in review by M. B. Bayly, G. Oertel, T. E. Tullis and D. S. Wood.

REFERENCES

Cobbold, P. R. 1976. Mechanical effects of anisotropy during large finite deformations. *Bull. Soc. geol. Fr.* **7**, 1497–1510.

Hobbs, B. E., Means, W. D. & Williams, P. F. 1982. The relationship between foliation and strain. An experimental investigation. *J. Struct. Geol.* **4**, 411–428.

March, A. 1932. Mathematische Theorie der Regelung nach der Korngestalt bei affiner Deformation. *Z. Kristallogr.* **81**, 285–298.

Means, W. D. 1975. Natural and experimental microstructures in deformed micaceous sandstone. *Bull. geol. Soc. Am.* **86**, 1221–1229.

Means, W. D., Hobbs, B. E., Lister, G. S. & Williams, P. F. 1980. Vorticity and non-coaxiality in progressive deformations. *J. Struct. Geol.* **2**, 371–378.

Oertel, G. & Wood, D. S. 1974. Finite strain measurement: a comparison of methods. *Eos (Trans. Am. Geophys. Un.)* **55**, 695.

Owens, W. H. 1972. Strain modification of angular density distributions. *Tectonophysics* **16**, 249–261.

Paterson, M. S. & Weiss, L. E. 1966. Experimental deformation and folding in phyllite. *Bull. geol. Soc. Am.* **77**, 343–374.

Ramberg, H. 1975. Particle paths, displacement, and progressive strain applicable to rocks. *Tectonophysics* **28**, 1–37.

Williams, P. F., Means, W. D. & Hobbs, B. E. 1977. Development of axial plane slaty cleavage and schistosity in experimental and natural materials. *Tectonophysics* **42**, 139–158.

Tullis, T. E. & Wood, D. S. 1975. Correlation of finite strain from both reduction bodies and preferred orientation of mica in slate from Wales. *Bull. geol. Soc. Am.* **86**, 632–638.

Wood, D. S., Oertel, G., Singh, J. & Bennett, H. F. 1976. Strain and anisotropy in rocks. *Phil. Trans. R. Soc.* **A283**, 27–42.